Low Spreading Loss in Underwater Acoustic Networks Reduces RTS/CTS Effectiveness

Jim Partan†* Jim Kurose* Brian Neil Levine* James Preisig†
*Dept. of Computer Science, University of Massachusetts, Amherst
partan@cs.umass.edu, kurose@cs.umass.edu, brian@cs.umass.edu
†Dept. of Applied Ocean Physics and Engineering, Woods Hole Oceanographic Institution
jpartan@whoi.edu, jpreisig@whoi.edu

ABSTRACT

The relatively low spreading losses in underwater acoustic channels allows increased interference from distant interferers, which reduces the effectiveness of collision-avoidance MAC protocols. These collisions in turn reduce spatial reuse and network goodput, and increase power consumption. A competing channel effect, however, is the frequency-dependent absorption. The absorption can strongly suppress distant interferers, improving the effectiveness of collision-avoidance protocols. A third channel effect is frequency-dependent ambient noise, which reduces effectiveness for links consisting of widely separated nodes. RTS/CTS effectiveness generally decreases with decreasing acoustic frequency.

We present analytic, numerical, and simulated results detailing how each of the major characteristics of the physical channel and physical layer affect the RTS/CTS effectiveness. We find that RTS/CTS effectiveness can drop to between 50%–90% for source and receiver separated by more than about two-thirds of the maximum packet range. The effect depends heavily on the acoustic frequency. We also present as a hypothesis an alternative physically based spreading model that distinguishes between desired signals, which are typically coherently detected via the largest of their multipath arrivals, and interfering signals whose effect on detection performance is related to the total energy in all of their multipath arrivals.

1. INTRODUCTION

Underwater wireless sensor networks for oceanographic applications rely on underwater acoustic communication at the physical layer. Underwater acoustic communication channels have a number of physical differences from terrestrial radio communication channels, including speed of propagation, spreading loss model, as well as frequency-dependent absorption and ambient noise. Previous work on RTS/CTS-based MAC protocols in the domain of underwater acoustic networks (UANs) has mostly focused on propagation delay issues. While RTS/CTS-based protocols are usually relatively inefficient due to large propagation delays [1,2], they are nevertheless being proposed for underwater acoustic networks, in part due to their practical simplicity [3–7].

In this paper, we analyze the effects of spreading losses, frequency-dependent absorption, and frequency-dependent ambient noise on collision-avoidance protocols derived from MACAW [8], i.e. using RTS/CTS/DATA/ACK handshakes. Specifically, we use analytic results, numerical results, and simulations to evaluate the effectiveness of RTS/CTS-based collision avoidance in UANs. The effectiveness of the collision avoidance protocol determines the degree to which spatial reuse is possible within the network. Previous work on UAN spatial reuse has dealt with TDMA and FDMA cellular architectures [9], rather than RTS/CTS-based ad hoc networks.

We build on previous work by Xu et al. [10] which argues that for 802.11-based radio networks, packets can cause collisions at ranges significantly larger than the range at which they can be detected. In this case, the RTS/CTS handshake cannot prevent all collisions, which reduces spatial reuse, network efficiency, and energy efficiency. The range at which interferers can cause collisions depends upon the distance between transmitter and receiver, the packet detection threshold, and the physical channel characteristics.

In UANs, physical waveguide effects in the communications channel reduce spreading losses significantly relative to radio channels. The small spreading loss allows interference from distant nodes. A competing physical effect is from absorption, which can suppress distant interferers strongly, improving spatial reuse. A third effect is that of ambient noise, which reduces the effectiveness of RTS/CTS collision avoidance for widely spaced nodes. Aside from spreading, these effects are frequency-dependent, and analyzing spatial reuse in UANs is a complex problem.

Our contributions in this paper include the following:

- We extend Xu et al.'s basic model to a simple channel model for UANs that considers spreading losses only. The properties of UANs invalidate one of their original assumptions, which we fix. The resulting solution suggests that on average, RTS/CTS handshakes begin to lose effectiveness in UANs for node separations of only 22% of the maximum range, versus about 56% for radio networks, for typical parameters.
- Using a more realistic channel model, we present numerical results for the RTS/CTS effectiveness, and also derive physically based analysis to explain how different communication parameters affect spatial reuse. These parameters include detection threshold, node separation, transmit power, absorption coefficients, and ambient noise power. We find that the strong effects from absorption improve spatial reuse for most intermediate node separations to approximately the level of collision-avoidance performance in RF networks.
- We hypothesize an mixed-exponent spreading model with different spreading exponents for signal and interference, as an alternative in certain situations to the widely accepted $k \approx 1.5$ spreading model, including when using high-bitrate PSK packets requiring coher-

ent detection. In such channels, RTS/CTS effectiveness would drop significantly, especially for low frequencies. For instance, at 3 kHz, on average the RTS/CTS handshake would suppress under 10% of potential interferers for all but the smallest node separations.

- We validate the numerical results from our analytical model with simulations incorporating the channel model, physical layer, and link-layer MAC protocols.

We conclude with a discussion of several possible methods for improving spatial reuse in UANs using RTS/CTS-based MAC protocols.

2. BACKGROUND

Our contributions extend a basic model of RF MAC-layer behavior by Xu et al. [10] (and Ye et al. [11]). Their study of RTS/CTS-based MAC protocols found that interference from nodes that are out of data communication range can cause collisions; that is, the interference range of transmissions is typically larger than the data range. In this section, we re-state their model and results, and in the next section, we extend the model to account for the physical properties of underwater acoustic communication channels.

Xu et al.'s analysis begins with the simple statement that collision avoidance requires the successful detection of RTS/CTS packets. In other words, it must be that

$$T \leq \text{SINR}, \tag{1}$$

where T is the receiver's detection threshold, and SINR is the signal-to-interference-and-noise ratio at the receiver. Following the notation introduced by Xu et al., let d be the distance between transmitter and receiver. Let r be the distance from receiver to the closest interferer. The simple model analyzed by Xu et al. does not include ambient noise and signal absorption, reducing SINR to SIR, the signal-to-interference ratio. The RF-based networks they study have a spreading exponent of $k \approx 4$ for a two-ray ground-reflection model [12]. In that case, Eq. 1 becomes

$$T \leq \text{SIR} = \frac{Pd^{-k}}{Pr^{-k}} = \left(\frac{r}{d}\right)^k \tag{2}$$

where P is the transmit power for all nodes. Choosing equality in Eq. 2 gives the minimum allowable distance r to the interferer such that the collision-avoidance between source and receiver is successful. Let this minimum allowable distance be denoted by R_i. Defining

$$\gamma = R_i/d \tag{3}$$

gives $\gamma = T^{1/k}$ for this simple channel model. We examine γ in greater detail in the next sections, extending it to a frequency-dependent form for more realistic channel models. We refer to γ as the *interference range ratio*, and it is the fundamental quantity of interest in this paper: it determines the effectiveness of the collision-avoidance protocol. For the simple model in this section, with spreading losses only, γ is a constant, which we denote by $\gamma_o = T^{1/k}$. In general, RTS/CTS effectiveness is higher when γ is lower.

Let R_{tx} be the maximum transmission range of all packets such that detection is successful. If $R_i \leq R_{\text{tx}}$, then the CTS packet will reach all potential interferers, and suppress their transmissions. If, however, $R_i > R_{\text{tx}}$, then some interferers will not be suppressed, leading to packet collisions.

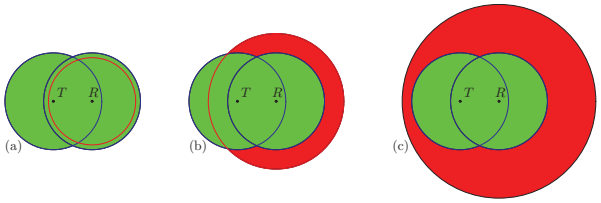

Figure 1: Three scenarios: (I) Interference range R_i is less than transmission range R_{tx}, and all potential interferers suppressed by the RTS/CTS handshake; (IIa) Some of the potential interferers are not suppressed by the RTS/CTS handshake (red); (IIb) Many potential interferers not suppressed (red).

The maximum separation of any two communicating nodes is when $d = R_{\text{tx}}$, and so if $\gamma > 1$, then R_i can be greater than R_{tx} for some nodes in the network. In this case, the collision-avoidance protocol is not fully effective. As R_i (or γ) increases, the number of potential interferers increases dramatically, roughly as R_i^2 for a 2-dimensional network deployment. (It is possible for UANs to be 3-dimensional [13], but most applications are in fact 2-dimensional deployments.) While it is well-known that wireless network nodes do not have a circular (or spherical) coverage region [14], and that UANs often have low node density, this approximation allows the physical analysis in this paper, offering theoretical insight into the protocol performance.

For RF wireless networks, setting $k = 4$ and $T = 10$ dB gives $\gamma_o = 1.8$. Even at this relatively small value of γ_o, Xu et al. and Ye et al. conclude that interference in RF networks can greatly reduce collision-avoidance protocol effectiveness.

Xu et al. also define the RTS/CTS effectiveness, $E_{\text{RTS/CTS}}$, as the fraction of the interference region that is covered by the collision-avoidance RTS/CTS handshake packets. In a 2-dimensional network deployment, assuming uniform node distribution and transmission times, this is a ratio of areas:

$$E_{\text{RTS/CTS}} = \frac{A_{(i \cap \text{RTS/CTS})}}{A_i}, \tag{4}$$

where A_i is the area in which there could be a potential interferer, $A_{\text{RTS/CTS}}$ is the area covered by the RTS/CTS collision avoidance protocol, and $A_{(i \cap \text{RTS/CTS})}$ is the intersection of these regions.

3. A SIMPLE INTERFERENCE MODEL

To extend the model to underwater acoustic channels, our first challenge is to account for the waveguide effects that result in much lower spreading exponents, often taken as so-called "practical spreading", with $k \approx 1.5$ [7, 15, 16]. For UANs, setting $k = 1.5$ and $T = 10$ dB gives $\gamma_o = 4.6$. Therefore, we see immediately that long-range interference can be a more significant problem in UANs than it is in RF networks.

While it would be easy to simply apply Eq. 2 for a different spreading exponent, applying Eq. 4 to underwater channels is requires additional work, as Xu et al.'s analysis made an approximation that does not apply to underwater channels.

3.1 RTS/CTS Effectiveness

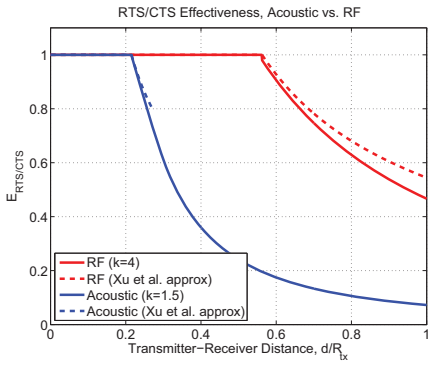

Figure 2: RTS/CTS effectiveness in underwater networks is hurt significantly by long-range interference. The dotted lines use the approximation in [10] and [11], and the solid lines use the equations derived in our tech report. The plot assumes $T = 10$ dB and no absorption or ambient noise.

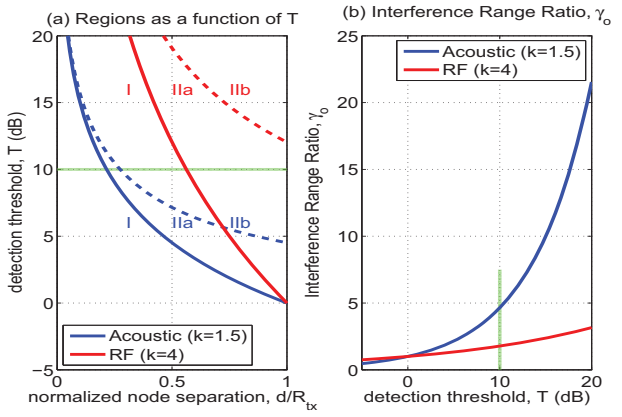

Figure 3: (a) Regions for Scenarios I, IIa, and IIb as a function of detection threshold (T on vertical axis). See Fig. 1 for scenario definitions. Dotted lines separate cases IIa and IIb. (b) Interference range ratio γ_o as a function of detection threshold T. In both (a) and (b), the green dashed line indicates $T = 10$ dB; the plots are valid only for no ambient noise and no absorption.

Fig 1 illustrates the three possible scenarios when comparing the distances of the source, receiver, and interferer:

I: $0 < R_i < R_{\text{tx}}$: the geographic range of CTS packets covers all potential interferers.

IIa: $R_{\text{tx}} < R_i < R_{\text{tx}} + d$: the range of CTS packets covers most of the area from which third parties can interfere.

IIb: $R_{\text{tx}} + d < R_i$: The range of CTS packets covers a small fraction of the area from which third parties can interfere.

Note that in RF networks with a detection threshold of $T < 12$ dB, Scenario IIb does not occur, and so it is not analyzed in previous work. Xu et al. and Ye et al. use an approximation for $A_{(i \cap \text{RTS/CTS})}$ based on an idealized circular geometry for wireless range that only is valid for Scenario IIa. When Scenario IIb does occur, as it will for most underwater networks, that approximation will lead to a discontinuity in $E_{\text{RTS/CTS}}$.

We derive a new calculation of $A_{(i \cap \text{RTS/CTS})}$, exact in this idealized case of circular transmission ranges, that is valid for all three scenarios; due to space limitations, the details are available only in a technical report [17]. For the simplified channel model (i.e., without considering absorption or ambient noise), we use the results from the tech report to plot $E_{\text{RTS/CTS}}$ for RF and underwater acoustic networks in Fig. 2. We set the detection threshold $T = 10$ dB, and use spreading exponents of $k = 4$ and $k = 1.5$, respectively. In Fig. 2, the dotted-line shows the values obtained by Xu et al.'s approximation, and the solid lines are the result of our exact calculation. Xu et al.'s results for acoustic networks end quickly as their assumptions become invalid and the calculation becomes discontinuous.

Fig. 2 replicates Xu et al.'s results, and extends them to a simple underwater acoustic channel model, with spreading losses only. In an RF network, when the source/receiver pair are in Scenario I (i.e., when d/R_{tx} is less than about 56% for $T = 10$ dB) then the RTS/CTS collision avoidance protocol is fully effective — all potential interferers are suppressed. For larger source-to-receiver separations, the RTS/CTS protocol becomes increasingly ineffective. For RF networks with detection threshold $T < 12$ dB, the network will always be in Scenarios I or IIa, as Fig. 3a illustrates graphically.

For UANs, however, with a typical spreading loss of $k = 1.5$ and detection threshold of $T = 10$ dB, then the RTS/CTS collision avoidance protocol starts losing effectiveness when d/R_{tx} is larger than about 22%. The collision-free region therefore covers less than 5% of the area within the maximum transmission range.

3.2 Effects of Detection Threshold on γ_o

Fig. 3b shows how the interference range, R_i, increases sharply with an increasing detection threshold, T in this model. For efficient RTS/CTS MAC protocols, it is therefore *important to minimize the packet detection threshold.*

Incoherent detection methods, such as detecting the start of the packet by detecting coded sequences of frequency-hopped FSK signals (FH-FSK), generally have low detection thresholds, which can be 3 dB or less [18]. These low detection thresholds will allow significant spatial reuse when using robust, low bitrate modulation and coding techniques for which timing synchronization requirements can be supported by FH-FSK or other low-SINR detection techniques.

Packets with higher bitrates generally use PSK modulation, and the detector needs to detect the start of the packet with higher time resolution than FH-FSK methods can provide [19]. Coherent detection methods, such as matched-filter detectors, typically require detection thresholds of around 10 dB (although increasing the matched filter's processing gain can reduce the detection threshold). The remainder of this paper assumes a detection threshold of 10 dB. With the higher time resolution, and hence higher detection thresholds, required for packets with higher bitrates, γ_o increases significantly as shown in Fig. 3b, reducing spatial reuse in the network.

4. AN EXTENDED INTERFERENCE MODEL

In the previous section, we were able to derive a closed form solution for γ_0 using a simple channel model. In this section, we introduce a more realistic underwater acoustic channel model. For this case, we are able to express our result as only a numerical solution.

Absorption losses vary strongly with frequency in UANs, and hence must be included in the channel model. Ambient noise from ships, wind-driven waves, rain, shrimp, etc. is a fundamental part of the natural acoustic environment and cannot be neglected. Following Stojanovic [16], we use Thorp's expression for the frequency-dependent acoustic energy absorption coefficient, $\alpha(f)$, which is generally expressed in dB per unit distance. To model ambient noise power, $\sigma_N(f)$, we use the empirical power spectral density (PSD) from Stojanovic [16], parameterized by a shipping factor of 0.5 and wind speed of 3 m/s. We integrate this PSD across a bandwidth of 1/3 of the center frequency, which is typical of acoustic transducers used in UANs.

For our spreading model, at first we again use the "practical spreading" model, with a spreading exponent of $k = 1.5$. In Section 5, we propose an alternate physically based spreading model that has lower spreading losses for interfering signals and higher spreading losses for signals that require detection.

We do not use transmit power control, and we use a fixed transmit power of 185 dB re:1μPa@1m, a typical value for underwater acoustic modems.

4.1 Calculating $\gamma(f, d)$

By including absorption and ambient noise, γ is no longer a constant. In this extended model, $\gamma(f, d)$ is a function of frequency f and source-receiver separation d. We start with the condition for detection $T \leq \text{SINR}$ (Eq. 1). This expression achieves equality for the minimum allowable SINR for detection, which occurs at the minimum allowable interferer range, R_i:

$$T = \text{SINR} = \frac{P_s\ S(d,k)\ A(f,d)}{P_i\ S(R_i,k)\ A(f,R_i) + \sigma_N(f)}. \qquad (5)$$

In this expression, the transmit powers for source and interferer are P_s and P_i, respectively. In all plots in this section, we set $P_s = P_i$. The spreading loss factor is $S(r,k) = (r/r_o)^{-k}$, where r_o is a reference distance, typically taken as $r_o = 1$ m. The absorption factor is $A(f,r) = 10^{-\alpha(f)r/10}$. The ambient noise power at the receiver is $\sigma_N(f)$. In this paper, we consider a single interferer at range R_i and idealized receivers. In practice, there are numerous complications [20].

Since $R_i = \gamma\, d$, then from Eq. 5, we have

$$\gamma^{-k}\,(A(f,d))^{(\gamma-1)} = \frac{P_s}{P_i T} - \frac{\sigma_N(f)}{P_i\ S(d,k)\ A(f,d)} \qquad (6)$$

In general, there is no closed-form solution of Eq. 6 for $\gamma(f, d)$. We solve this equation numerically, and we discuss the results below.

4.2 Effects of Ambient Noise and Absorption

Absorption and ambient noise add strong frequency-dependent effects to the interference range ratio, $\gamma(f, d) = R_i/d$. Fig. 4 shows $\gamma(f, d)$ for typical acoustic communication frequencies ranging from 3 kHz to 80 kHz for a spreading exponent of $k = 1.5$. Fig. 4a shows $\gamma(f, d)$ *without* ambient noise, while Fig. 4b shows $\gamma(f, d)$ *with* ambient noise, to help distinguish

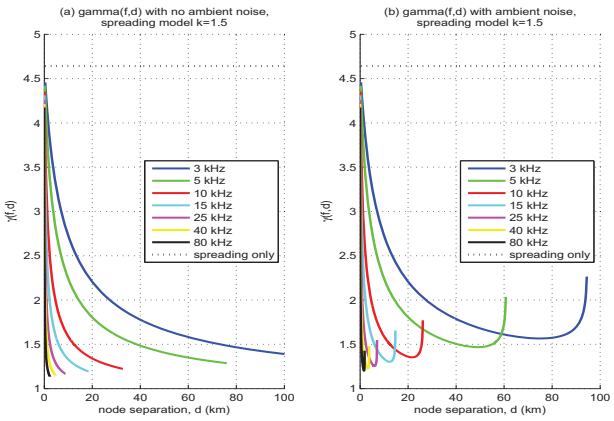

Figure 4: Numerical solutions for $\gamma(f, d)$ for the spreading model $k = 1.5$, with absorption, for several frequencies. (a) is without ambient noise; (b) includes ambient noise. The dashed lines show comparisons with the case of spreading losses only.

the effect of each. We examine the results in three parts: small, intermediate, and large node separations.

For small node separations, spreading losses dominate. In that case, absorption and ambient noise can be neglected, and γ approaches γ_o. This effect can be seen in both Figs. 4a and 4b.

For intermediate node separations, absorption losses dominate and largely determine the shape of the $\gamma(f, d)$ curves in Fig. 4. If we neglect ambient noise (letting $\sigma_N(f) = 0$), and focus on the intermediate separation distances, we can ignore the spreading term γ^{-k} in Eq. 6. In that case, intermediate node separations can be described as

$$\gamma(f,d) \approx 1 + \left(\frac{10\log_{10}(T)}{\alpha(f)}\right)\ \frac{1}{d}. \qquad (7)$$

Spreading losses are polynomial in range, whereas absorption losses are exponential in range (i.e., for range r, spreading losses scale as r^{-k}, and absorption losses scale as $10^{-\alpha(f)r/10}$). For all but the smallest node separations, therefore, this intermediate case applies, and $\gamma(f, d)$ scales as $1/d$ in this region.

When node separations are large and approach the maximum transmission range, ambient noise starts to affect $\gamma(f, d)$ significantly. This effect can be seen by comparing Figs. 4a and 4b.

The maximum transmission range is when no interferers are present, so the signal-to-noise ratio equals the detection threshold, i.e., $T = \text{SNR}$. In that case, R_{tx} is the numerical solution of Eq. 5, with $P_i = 0$:

$$\left(\frac{R_{\text{tx}}}{r_o}\right)^{-k} A(f,R_{\text{tx}}) = \frac{T\,\sigma_N(f)}{P_s}. \qquad (8)$$

For node separations that approach the maximum transmission range, even a small amount of interference will prevent detection. As the node separation approaches the maximum transmission range, the minimum allowable distance from the receiver to an interferer for successful detection approaches infinity. So, when ambient noise is included in the model, $\gamma(f, d)$ approaches infinity as the node separation approaches

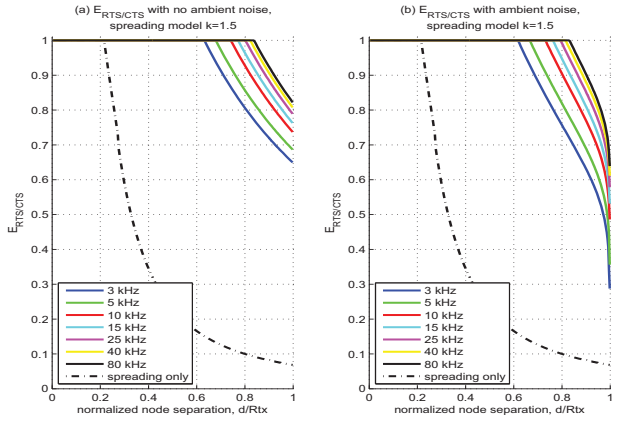

Figure 5: $E_{\text{RTS/CTS}}$, calculated with $\gamma(f,d)$ from Fig. 4 for several frequencies, with spreading and absorption losses. (a) is without ambient noise, while (b) includes ambient noise. The dashed lines show comparisons with the case of spreading losses only.

the maximum transmission range.

One way to avoid the susceptibility of widely separated nodes to ambient noise is to set the UAN's routing tables so that packets are not routed on links whose node separation approaches the maximum transmission range. This is a caveat to the general idea that one should route over long hops in a wireless network [21].

The competing effects of absorption and ambient noise lead to the minimum in $\gamma(f,d)$ apparent in Fig. 4b.

4.3 RTS/CTS Effectiveness with Absorption and Ambient Noise

The RTS/CTS MAC protocol can avoid all collisions only if all potential interferers can detect the RTS or CTS successfully. Since interference occurs at the receiver, it is especially important that a potential interferer can detect the CTS packet. Section 2 introduces the RTS/CTS effectiveness metric, $E_{\text{RTS/CTS}}$. We can derive expressions for $E_{\text{RTS/CTS}}$ and the regimes of node separations over which each expression applies (not shown, but see Fig. 3a). Given a node separation d, we can calculate the interference range, $R_i = \gamma(f,d)\,d$, where $\gamma(f,d)$ is the numerical solution of Eq. 6, plotted in Fig. 4. From Eq. 8, we can calculate the maximum transmission range, R_{tx}.

In the expressions for $E_{\text{RTS/CTS}}$, the terms $A_i = \pi R_i^2 = \pi\gamma^2 d^2$, and both $A_{\text{RTS/CTS}}$ and $A_{(i\cap\text{RTS/CTS})}$, are derived analytically in our technical report [17]. We can then calculate $E_{\text{RTS/CTS}}$ for a given frequency f as a function of node separation d, up to the maximum node separation, R_{tx}. This function is plotted in Fig. 5.

Since the absorption reduces $\gamma(f,d)$ compared with the spreading-only case, $E_{\text{RTS/CTS}}$ is improved compared with the spreading-only case, as shown in Fig. 5. When ambient noise is included, $E_{\text{RTS/CTS}}$ drops for node separations which approach the maximum transmission range, shown in Fig. 5b. Effectiveness is lower for lower acoustic frequencies.

We have analyzed the effect of detection threshold on $\gamma(f,d)$ in the channel extended model, and the results are in the technical report [17]. In short, $\gamma(f,d)$ increases rapidly with an increasing detection threshold.

5. MIXED-EXPONENT SPREADING MODEL

The so-called "practical spreading" approximation of $k \approx 1.5$ is a widely used spreading model for point-to-point underwater communication links [15]. The details of the spreading model are generally not significant in point-to-point acoustic communications research, but *the spreading model is significant for understanding interference in a network*. As we discuss below, in the case of detecting high-bitrate packets in a UAN, we hypothesize that an alternate spreading model with different spreading exponents for signal and interference, may be more appropriate than the "practical spreading" model. We have observed the validity of different spreading exponents for signal and interference in numerical modeling but have not yet validated it with field data.We present results showing that, if the mixed-exponent spreading model is in fact valid, the RTS/CTS effectiveness can be very low, especially for UANs transmitting on low frequencies.

The $k \approx 1.5$ "practical spreading" model is not solidly grounded, but has been considered adequate for underwater acoustic communications because other physical channel effects are much more significant, though this is not necessarily true at the network layer. Energy from a point source transmitter in an idealized channel of very deep, uniformly mixed water will experience spherical spreading, such that $k \approx 2$. In most situations, however, multipath effects from either shallow water reflections or a deep-water refractive sound channel will lead to waveguide effects reducing the effective spreading exponent. In the idealized case of shallow water with a perfectly reflecting surface and bottom, the *incoherent* sum of the energy from a point source will experience cylindrical spreading, such that $k \approx 1$, at large ranges relative to the water depth. The practical spreading model with $k \approx 1.5$ is a combination of these two regimes.

5.1 Signal and Interference Spreading

In our hypothesized model, we assign separate spreading exponents to signal and interference. The basic intuition for the difference is that many receivers (such as the WHOI Micromodem-1 [22]) process signal and interference differently when detecting the start of a packet (aside from multiuser receivers, which traditionally have had high computational complexity [23]). This difference may effectively increase the spreading exponent for signals and decrease it for interference.

Signal spreading. For FH-FSK communication, which typically has low bitrates, packet detectors can be incoherent energy detectors, generally detecting on FH-FSK tone patterns, with low time resolution. Higher bitrates generally require PSK modulation or OFDM. PSK requires a precise time synchronization on the start-time of the packet, while OFDM requires precise frequency synchronization [24].

For PSK packets, *coherent* detectors, such as matched-filter detectors, detect on a known signal at the start of the packet, and they provide the precise timing measurements required for these high-bitrate packets. This initial detection is before the receiver's adaptive equalizer has been trained, and so the initial detection typically detects on just a *single* multipath arrival. When detecting the start of high-bitrate data packets, the signal's effective spreading loss is the spreading loss experienced by a single multipath arrival, and accordingly $k_s \approx 2$; here, the subscript s is for signal.

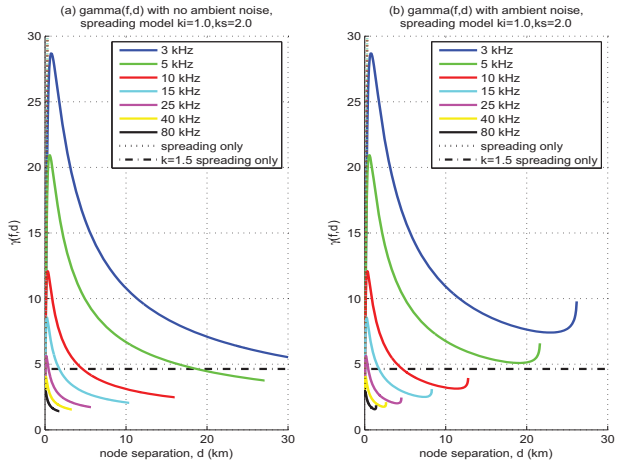

Figure 6: Numerical solutions for $\gamma(f,d)$ for the hypothesized spreading model $k_i = 1$, $k_s = 2$, with absorption, for several frequencies. (a) is without ambient noise; (b) includes ambient noise.

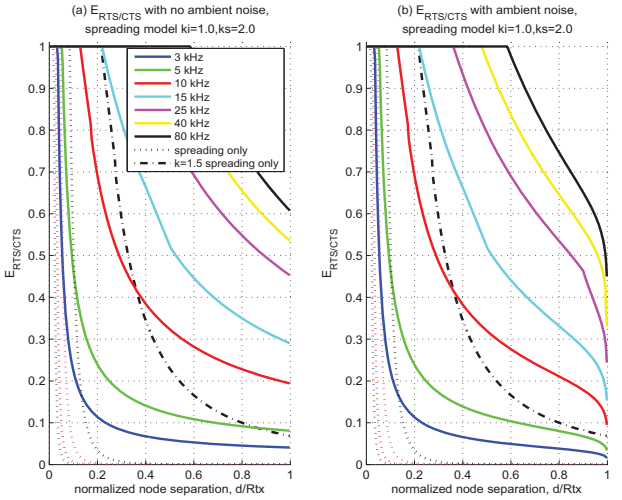

Figure 7: $E_{\mathrm{RTS/CTS}}$, calculated with $\gamma(f,d)$ from Fig. 6, with absorption losses and hypothesized mixed-exponent spreading model. (a) is without ambient noise, while (b) includes ambient noise. The dashed lines show comparisons with the case of spreading losses only: the $k = 1.5$ spreading model in dashes, and the $k_i = 1$, $k_s = 2$ in dots (varying among frequencies due to the different maximum detection ranges, but with the same water depth; see Eq. 11).

Beyond a certain range, however, separate multipath arrivals become unresolvable, and they *coherently* combine in the received signal. This is the region in which the signal spreading transitions from a spherical-spreading regime ($k_s \approx 2$) to a cylindrical-spreading regime ($k_s \approx 1$). This range increases with bandwidth and the water's depth.

With an OFDM system, the overall bandwidth is divided into many small sub-bands, in contrast to a single band for a PSK system. Therefore, for each sub-band, the range at which k_s transitions from spherical to cylindrical spreading would be smaller with OFDM compared with PSK, if the mixed-exponent spreading model is valid. This would improve the RTS/CTS effectiveness for OFDM-based systems relative to PSK-based systems.

Detection generally is the limiting factor for most packets, since the error-correction coding can be designed appropriately so that essentially all detected packets can be decoded successfully.

Interference spreading. In contrast, the interference received via all multipath arrivals combines to degrade the detection of desired signals. Modeling separate multipath arrivals as uncorrelated, the energy from these arrivals is combined incoherently to determine the interference level. A physically based model for the interference spreading loss is

$$S(r, w_d, k_i) = \begin{cases} \left(\frac{r}{r_o}\right)^{-2} & r < w_d \\ \left(\frac{w_d}{r_o}\right)^{-2} \left(\frac{r}{w_d}\right)^{-k_i} & r \geq w_d \end{cases} \qquad (9)$$

where r is the range from transmitter to receiver (ignoring slant range for the time being), w_d is the water depth, r_o is a reference distance (typically 1 m), and $k_i \approx 1$ is the spreading exponent for interference for ranges larger than the water depth. Similarly, we also use this model for signal spreading loss, $S(r, r_T, k_s)$, with the complication that k_s transitions from $k_s \approx 2$ to $k_s \approx 1$ beyond a transition range r_T. We have omitted this transition in our numerical results.

5.2 Implications for $\gamma(f,d)$ and $E_{\mathrm{RTS/CTS}}$

To use the hypothesized interference spreading model from Eq. 9, we adjust Eq. 5 slightly.

$$T = \mathrm{SINR} = \frac{P_s\ S(d, w_d, k_s)\ A(f,d)}{P_i\ S(R_i, w_d, k_i)\ A(f, R_i) + \sigma_N(f)} \qquad (10)$$

We can then numerically solve for $\gamma(f,d)$ as before. The water depth now appears explicitly in the spreading model. For the results in Figs. 6 and 7, we use a shallow-water environment of $w_d = 100$ m, since shallow water is often the situation of most interest for littoral military operations as well as coastal environmental monitoring.

The notable differences between Figs. 4 and 6 are that there now is a maximum $\gamma(f,d)$ value for small node separations, and that maximum can be much larger than the $\gamma(f,d)$ values for $k_i = k_s = 1.5$. For large node separations, Figs. 4 and 6 are qualitatively similar, though in Fig. 6, $\gamma(f,d)$ remains quite large even for large node separations.

We can provide an intuitive physical explanation for the maximum in $\gamma(f,d)$, deriving its location and amplitude in terms of physical parameters of the communications channel.

For small node separations, we can ignore ambient noise. Then with the alternate spreading model, Eq. 6 from the previous section becomes

$$\gamma^{-k_i}\ (A(f,d))^{\gamma-1} = \frac{P_s}{P_i T} \left(\frac{d}{w_d}\right)^{(k_i - k_s)} \qquad (11)$$

For very small node separations, we can also ignore absorption losses. In the case of very small node separations, setting $k_i = 1$ and $k_s = 2$, we have

$$\gamma \approx \left(\frac{P_i T}{P_s} \frac{d}{w_d}\right). \qquad (12)$$

Therefore, for very small node separations, $\gamma(f,d)$ increases

approximately linearly with node separation, up to a maximum. This maximum occurs when spreading losses balance with absorption losses. When the absorption losses dominate, then $\gamma(f,d)$ drops sharply, as explained in Section 4.

To find the maximum, $\gamma_{\max} = \gamma(f, d_{\max})$, we differentiate Eq. 11 with respect to d, and set the derivative of γ equal to zero. From Fig. 6 we can see that $\gamma_{\max}$ is relatively large (so for this analytical derivation we approximate $\gamma_{\max} \gg 1$), and the maximum occurs for small $d_{\max}$ (and so $A(f, d_{\max}) \approx 1$). Setting $k_i = 1$, $k_s = 2$, these approximations give

$$d_{\max} \approx \beta \left(\frac{P_s}{TP_i} \frac{w_d}{\alpha(f)} \right)^{1/2}, \tag{13}$$

where $\beta = (10 \log_{10}(\exp(1)))^{1/2}$. Plugging this value for $d_{\max}$ back into Eq. 12 gives an overestimate for $\gamma_{\max}$, since $\gamma(f,d)$ is convex in the neighborhood of its maximum:

$$\gamma_{\max} \approx \beta \left(\frac{TP_i}{P_s} \frac{1}{w_d \, \alpha(f)} \right)^{1/2}. \tag{14}$$

This result gives an intuition for which physical parameters control the amplitude and location of the maximum in $\gamma(f,d)$.

With this hypothesized mixed-exponent spreading model, $\gamma(f,d)$ obtains much higher values than it does with the "practical spreading" model. As a result, we see significantly lower RTS/CTS efficiency, as shown in Fig. 7b. For low frequencies, the MAC efficiency is particularly low. The plot shows center frequencies as low as 3 kHz. These are realistic frequencies for actual UANs; for instance, the PLUSNet deployment [25] includes a long-range channel with a center frequency of about 3 kHz.

One implication of Fig. 7b is that for multiband UANs [4, 25], different bands might use different MAC protocols. For certain deployments, RTS/CTS effectiveness might be considered acceptable on a high-frequency band, which would have small node separations, reducing the propagation delays. But it might be unacceptable for the low-frequency bands, with long node separations and the double penalty of low $E_{\text{RTS/CTS}}$ due to spreading effects, and low throughput due to propagation delays.

6. SIMULATIONS

To validate our numerical results, we extended the Castalia/OMNET++ simulator (`http://castalia.npc.nicta.com.au`) to include the underwater acoustic physical channel model described above, with spreading, absorption, and ambient noise. Absorption is simulated according to Thorp's expression, and we parameterize noise by the same values as in Section 4, using the empirical PSD in Stojanovic [16].

The main goal of the simulations was to calculate $\gamma(f,d)$, and therefore the key measurement is the interference range, R_i. By definition, any interferer within the interference range will prevent packet detection, preventing the RTS/CTS handshake from completing.

To measure the minimum allowable interference range, we ran simulations with three nodes. Node 1 and node 2 were a source and receiver pair. They attempted to complete RTS/CTS/DATA/ACK data transfer handshakes, with node 2 receiving the DATA packet. The third node was placed co-linearly with the first two nodes, with the receiver node in the center. Node 3 transmitted an interfering data packet with a duration equal to the length of the simulation. Node 3 started at a very large separation where it did not

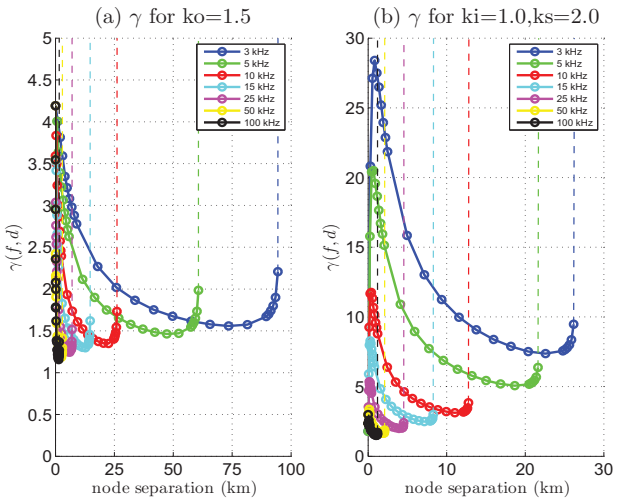

Figure 8: Simulation results for $\gamma(f,d)$. Note distinct x- and y-axes for the two plots. Compare against Figs. 4b and 6b, respectively, which cross validate the simulation and numerical results.

affect packet detection at Node 2, and gradually moved closer until its interference prevented packet detection at Node 2.

The parameters for a simulation run included the following. (1) The frequency f of the transmitted data and interference packets. We varied f from 3 kHz to 100 kHz, closely matching the analytical plots. (2) The spreading model. Using Equation 9, in one group of runs, we set $k_s = k_i = 1.5$; in the second, we set $k_s = 2.0$ and $k_i = 1.0$. (3) The separation distance d of the source and receiver pair (labeled *node separation* on the x-axis) (4) The distance r between the interfering node and receiver. (5) Communication channel parameters such as detection threshold and fixed transmit power, as in Section 4.

For each frequency f and source-receiver separation d, we ran simulations where Node 3 gradually reduced its interferer-receiver separation r. The last value of interferer range r for which the RTS/CTS/DATA/ACK transaction between Nodes 1 and 2 succeeded gives and estimate of γ, i.e. $\hat{\gamma} = r(\text{last success})/d$.

The results in Figure 8a should be compared against Figure 4b. Figure 8b should be compared against Figure 6b. Both simulation results agree well with the numerical results.

7. IMPROVING SPATIAL REUSE

The main approaches to improving spatial reuse primarily center on increasing the range of the RTS/CTS handshake. While extending the range of the RTS suppresses other nodes needlessly, a CTS control packet with range equal to the interference range would suppress only potential interferers.

Successful detection is usually the limiting factor for the range of a packet when the error-correcting coding is designed appropriately. To increase the range of a packet with a fixed detection threshold T, we need to increase the SINR at the receiver for the start-of-packet synchronization signal. This is usually done by increasing the transmitter power or by increasing the time duration of the synchronization signal. Alternately, the frequency band of the packet might

be shifted, either to a band with less absorption (lower frequencies) or to a band with less ambient noise (generally higher frequencies). At higher frequencies of about 40kHz, typical transducer bandwidths (with quality factor $Q \approx 3$) are wide enough to effectively allow a shorter-range channel (for data and RTS) and a longer-range channel (for CTS) with a single transducer, which might be a future possibility.

In extending the range of the CTS signal, the only information that needs to be transmitted to potential interferers is the single bit that a reception is about to occur within their interference range. The interferers do not necessarily need to decode any other information from the CTS header. This might lend itself to a very practical implementation for existing acoustic modems: right before transmitting a CTS packet, transmit a signal with high processing gain (and hence longer range). Any node detecting the CTS signal would enter a quiet backoff state, just as if it had received the CTS packet itself. This would not require any changes to the existing hardware, and would not change either the transmit power or the frequency band.

Another approach is to implement transmitter power control. This approach improves spatial reuse, reduces energy consumption, and reduces the probability of detection for covert communication. Linear power amplifiers are not as power-efficient as clipped ("Class D") power amplifiers, which are the standard power amplifiers for many UANs [22]. Pulse-width modulation (PWM) amplifiers are becoming more common and more power efficient, however, and may solve many of these problems for future underwater acoustic modems.

8. CONCLUSION

Our results demonstrate that RTS/CTS efficiency in UANs is subject to frequency-dependent effects and long-range interference, and not simply acoustic propagation delays.

We present a closed-form solution for γ_0 in a simple channel model, and a numerical solution for $\gamma(f, d)$ in an extended channel model. Our results show, for the practical spreading model, that both acoustic networks and RF networks have similar performance predictions, despite dramatically different channel models. In both cases, RTS/CTS effectiveness can drop to between 50%–90% for source and receiver separated by more than about two-thirds of the maximum packet range, depending on the frequency in the underwater acoustic case. Under the mixed-exponent spreading model, we predict that RTS/CTS effectiveness drops significantly. For example, for the 3 kHz deployment of PLUSNet, RTS/CTS effectiveness would quickly drop to 10% after source and receiver were separated by only 20% of signal range. Finally, we validated our analytical models using a physical simulation and found they matched quantitatively.

9. ACKNOWLEDGEMENTS

This material is based upon work supported by the National Science Foundation under Award CNS-0519881, as well as Office of Naval Research Grants N00014-05-10085 and N00014-07-10738. Any opinions, findings, and conclusions or recommendations expressed in this material are those of the authors and do not necessarily reflect the views of the National Science Foundation.

10. REFERENCES

[1] J.Heidemann, W.Ye, J.Wills, A.Syed, and Y.Li. Research Challenges and Applications for Underwater Sensor Networking. In *Proc. IEEE WCNC*, 2006.

[2] I. Akyildiz, D. Pompili, and T. Melodia. Challenges for efficient communication in underwater acoustic sensor networks. *SIGBED Rev.*, 1(2):3–8, July 2004.

[3] X. Guo, M. R. Frater, and M. J. Ryan. Design of a Propagation-delay-tolerant MAC Protocol for Underwater Acoustic Sensor Networks. *IEEE J. Oceanic Engineering*, 34(2):170–180, Apr 2009.

[4] S. Shahabudeen, M. Chitre, and M. Motani. A multi-channel MAC protocol for AUV networks. In *Proc. IEEE Oceans Europe*, June 2007.

[5] M. Molins and M. Stojanovic. Slotted FAMA: A MAC Protocol for Underwater Acoustic Networks. In *Proc. IEEE OCEANS Conf.*, Sept 2006.

[6] B.Peleato and M.Stojanovic. A MAC protocol for ad hoc underwater acoustic sensor networks. In *WUWNet*, 2006.

[7] E. Sözer, M. Stojanovic, and J. Proakis. Underwater Acoustic Networks. *IEEE J.Oceanic Eng.*, 25(1):72–83, 2000.

[8] V. Bharghavan, A. Demers, S. Shenker, and L. Zhang. MACAW: a media access protocol for wireless LANs. In *Proc. ACM SIGCOMM*, pages 212–225, Oct. 1994.

[9] M.Stojanovic. Frequency reuse underwater: capacity of an acoustic cellular network. In *WUWNet*, 2007.

[10] K.Xu, M.Gerla, and S.Bae. Effectiveness of RTS/CTS handshake in IEEE 802.11 based ad hoc networks. *Ad Hoc Networks*, 2003.

[11] F.Ye, S.Yi, and B.Sikdar. Improving Spatial Reuse of IEEE 802.11 Based Ad hoc Networks. In *GLOBECOM*, 2003.

[12] T.S. Rappaport. *Wireless Communications: Principles and Practice*. Prentice Hall, 1996.

[13] D.Pompili, T.Melodia, and I.Akyildiz. Routing algorithms for delay-insensitive and delay-sensitive applications in underwater sensor networks. In *Proc. MobiCom*, Sept 2006.

[14] D. Kotz, C. Newport, R. Gray, J. Liu, Y. Yuan, and C. Elliott. Experimental Evaluation of Wireless Simulation Assumptions. In *IEEE MSWiM*, pages 78–82, Oct 2004.

[15] Rodney F. W. Coates. *Underwater Acoustic Systems*. Halsted Press, 1989.

[16] M.Stojanovic. On the Relationship Between Capacity and Distance in an Underwater Acoustic Communication Channel. *ACM SIGMOBILE MC2R*, 11(4):34–43, Oct 2007.

[17] J. Partan, J. Kurose, B. Levine, and J. Preisig. Spatial Reuse in Underwater Acoustic Networks using RTS/CTS MAC Protocols. Technical Report UM-CS-2010-045 `www.cs.umass.edu/publication/details.php?id=2047`, University of Massachusetts Amherst, 2010.

[18] J.C. Preisig and M.P. Johnson. Signal detection for communications in the underwater acoustic environment. *IEEE J. Oceanic Engineering*, 26(4):572–585, 2001.

[19] M. Stojanovic. Recent Advances in High-Speed Underwater Acoustic Communications. *IEEE J. Oceanic Engineering*, 21(2):125–136, Apr. 1996.

[20] D.Son, B.Krishnamachari, and J.Heidemann. Experimental study of concurrent transmission in wireless sensor networks. In *Proc. ACM SenSys*, 2006.

[21] D.Aguayo, J.Bicket, S.Biswas, G.Judd, and R.Morris. Link-level measurements from an 802.11b mesh network. In *Proc. ACM SIGCOMM*, Aug 2004.

[22] L.Freitag, M.Grund, S.Singh, J.Partan, P.Koski, and K.Ball. The WHOI Micro-Modem: An Acoustic Communications and Navigation System for Multiple Platforms. In *Proc. IEEE OCEANS*, Sept. 2005.

[23] E.Calvo and M.Stojanovic. Efficient Channel Estimation Based Multiuser Detection for Underwater CDMA System. *IEEE J. Oceanic Engineering*, 33(4):502–512, Oct 2008.

[24] M. Stojanovic. Low Complexity OFDM Detector for Underwater Acoustic Channels. In *Proc. IEEE OCEANS*, Sept 2006.

[25] M. Grund, L. Freitag, J. Preisig, and K. Ball. The PLUSNet Underwater Communications System. In *Proc. IEEE OCEANS*, Sept 2006.